

000 001 002 003 004 005 006 007 008 009 010 011 012 OVERSMOOTHING, “OVERSQUASHING”, HETEROPHILY, LONG-RANGE, AND MORE: DEMYSTIFYING COMMON BELIEFS IN GRAPH MACHINE LEARNING

013
014
015
016
017
018
019
020
021
022
023
024
025
026
027
028
029
030
031
032
033
034
035
036
037
038
039
040
041
042
043
044
045
046
047
048
049
050
051
052
053
Anonymous authors

Paper under double-blind review

ABSTRACT

After a renaissance phase in which researchers revisited the message-passing paradigm through the lens of deep learning, the graph machine learning community shifted its attention towards a deeper and practical understanding of message-passing’s benefits and limitations. In this paper, we notice how the fast pace of progress around the topics of oversmoothing and oversquashing, the homophily-heterophily dichotomy, and long-range tasks, came with the consolidation of commonly accepted beliefs and assumptions that are not always true nor easy to distinguish from each other. We argue that this has led to ambiguities around the investigated problems, preventing researchers from focusing on and addressing precise research questions while causing a good amount of misunderstandings. Our contribution wants to make such common beliefs explicit and encourage critical thinking around these topics, supported by simple but noteworthy counterexamples. The hope is to clarify the distinction between the different issues and promote separate but intertwined research directions to address them.

1 INTRODUCTION

The last decade has seen an increasing scholarly interest in machine learning for graph-structured data (Sperduti & Starita, 1997; Micheli & Sestito, 2005; Gori et al., 2005; Bacciu et al., 2020). After an initial focus on the design of various message-passing architectures (Gilmer et al., 2017), inheriting from the recurrent Scarselli et al. (2009) and convolutional (Micheli, 2009) Deep Graph Networks (DGN), together with the analysis of their expressive power (Xu et al., 2019; Morris et al., 2023), researchers later turned their attention to the intrinsic limitations of the message-passing strategy and the relation between the graph, the task, and the attainable performance. We refer, in particular, to the fact that node embeddings may become increasingly similar to each other as more message-passing layers are used (Rusch et al., 2023), the loss of information that results from aggregating too many messages onto a single node embedding (Alon & Yahav, 2021), the presence of topological bottlenecks (Topping et al., 2022), the existence of neighbors of different classes Wang et al. (2024), and the propagation of information between far ends of a graph Dwivedi et al. (2022). Addressing these limitations makes a difference when applying message-passing models, including foundational ones Beaini et al. (2024), to large and topologically varying graphs at different scales, from proteins with hundreds of thousands of atoms (Zhang et al., 2023) to dynamically evolving social networks (Longa et al., 2023) with billions of users, where such limitations manifest together.

A pace of research so rapid can sometimes lead, however, to the premature consolidation of ideas and beliefs that have not been thoroughly verified. There are several reasons for this to happen: the (perhaps too) intense pressure to publish, follow the latest scientific trends, and demonstrate state-of-the-art performance. As a result, we may end up putting the spotlight on positive findings but overlooking contradictory evidence, eventually accepting hypotheses as canon.

In this paper, we argue and provide evidence that this is potentially the case for the afore-mentioned issues of *oversmoothing* (OSM), *oversquashing*¹ (OSQ), *heterophily*, and *long-range dependencies*, driving researchers away by the difficulty of circumventing common beliefs while concurrently introducing novel contributions. Scientific progress is therefore slowed down both in terms of reduced

¹We discuss and address the troubling abuse of the term “oversquashing” in later sections.

054
055
056
057
058
059
060
061
062
063
064
065
066
067
068
069
070
071
072
073
074
075
076
077
078
079
080
081
082
083
084
085
086
087
088
089
090
091
092
093
094
095
096
097
098
099
100
101
102
103
104
105
106
107
Table 1: List of common beliefs. For a non-exhaustive list of papers that make those claims, please refer to Table 2 in the Appendix.

	Beliefs	Beliefs
OSM	1. OSM is the cause of performance degradation. 2. OSM is a property of all DGNs.	6. OSQ synonym of a topological bottleneck. 7. OSQ synonym of computational bottleneck.
Hom-Het	3. Homophily is good, heterophily is bad. 4. Long-range propagation is evaluated on heterophilic graphs. 5. Different classes imply different features.	8. OSQ problematic for long-range tasks. 9. Topological bottlenecks associated with long-range problems.

workforce and clarity of the problems to be addressed; failure to acknowledge existing inconsistencies may well lead to a reiterated spreading of questionable claims.

While reviewing the literature, we identify and isolate **nine common beliefs** that, in our opinion, cause great confusion and ambiguities in the field. We then demystify such beliefs by providing *simple* and possibly memorable counterexamples that should be easy to recall. By encouraging critical thinking around these issues and separating the different research questions, we hope to foster further advancements in the graph machine learning field.

Disclaimer: We remark that the goal of this paper is not explicitly pinpointing criticalities in previous works; on the contrary, these works were fundamental to forming our current understanding and ultimately producing this manuscript. We also acknowledge that the list of referenced works cannot be exhaustive, due to the field’s size, and it mainly serves to support our arguments.

Table 1 summarizes our findings about common beliefs in the literature, together with the list of papers where we could find mentions of them². We logically divide common beliefs about OSM, OSQ, and the homophily-heterophily dichotomy. In the following sections, we discuss each belief, provide counterexamples, and summarize our arguments with take-home messages.

For readers that are less familiar with the topic and its definitions, Appendix B.1 provides a brief introduction to message-passing models.

2 IS OVERSMOOTHING REALLY A PROBLEM?

Oversmoothing broadly refers to the phenomenon where, as we stack more message-passing layers in a DGN, the node embeddings become increasingly similar to each other eventually collapsing into a low-dimensional (Huang et al., 2020; Oono & Suzuki, 2020)—or even single-vector (Cai & Wang, 2020)—subspace. This creates an almost constant representation, independent of the original node-feature distribution, and can **potentially** result in loss of discriminative power along the way (Li et al., 2018; Cai & Wang, 2020; Oono & Suzuki, 2020).

Formally, let $H^\ell \in \mathbb{R}^{n \times d}$ be the matrix of node embeddings after ℓ message-passing layers in a DGN, where n is the number of nodes and d is the hidden dimension. Consider a similarity (or separation) function $\pi: \mathcal{H} \rightarrow \mathbb{R}$, where $\mathcal{H} = \mathbb{R}^{n \times d}$ is the space of all possible embedding matrices. We say that a DGN experiences OSM if

$$\lim_{\ell \rightarrow \infty} \pi(H^\ell) = c. \quad (1)$$

where c is some constant indicating a collapse of embeddings. Deviation metrics (e.g., Dirichlet Energy (Cai & Wang, 2020), MAD Chen et al. (2020a)) and subspace-collapse criteria (Oono & Suzuki, 2020; Huang et al., 2024; Roth & Liebig, 2024) all measure the same intuition: as depth increases, node embeddings shrink toward a nearly constant subspace or degree-proportional vectors.

2.1 BELIEF: OSM IS A PROPERTY OF ALL DGNS.

A widespread claim in the literature is that *OSM happens regardless of the specific architecture or the underlying graph*. Early theoretical works support this view by analyzing message-passing

²Sometimes we found overly general claims in the first sections, later refined, which nonetheless contribute to the spreading of common beliefs.

108 propagation as a diffusion process: iterated normalized-Laplacian updates converge to a degree-
 109 weighted stationary distribution (Cai & Wang, 2020; Giraldo et al., 2023), while heat-kernel diffusion
 110 converges to a constant vector (Oono & Suzuki, 2020; Arnaiz-Rodriguez & Velingker, 2024). The
 111 resulting bounds quantify the rate of OSM in terms of the singular values of the feature transform W
 112 and the eigenvalues of the graph structure G .

113 These conclusions, however, rely on restrictive assumptions. Later work has relaxed them by intro-
 114 ducing learnable feature transforms, non-linear activations, and more elaborate architectures (Oono
 115 & Suzuki, 2020; Cai & Wang, 2020; Wu et al., 2023a), yet no existing proof shows inevitable
 116 collapse under realistic training regimes. In practice, remedies such as residual/skip connections,
 117 normalization layers, or gating mechanisms are explicitly architectural changes designed to maintain
 118 local distinctions, calling into question the universality of this OSM claim.

119 In addition, many studies probe OSM with *untrained* (weights frozen at initialization) linear GCN
 120 stacks, an experimental choice that hides the effect of learning and may lead to the wrong conclu-
 121 sions, as noted by Zhang et al. (2025). Indeed, Cong et al. (2021, Figure 2) report OSM only for
 122 frozen-weight networks; once parameters start adapting, the models preserve informative variance.

123 Together, these observations suggest that OSM is not an inevitable consequence of message-passing
 124 but rather a contingent outcome that depends on training dynamics and architectural design choices.

125 **Empirical Example** We show a simple training scenario where we see how OSM is *not* a property
 126 of all DGNs and how different elements make it difficult to draw clear conclusions. We train several
 127 DGNs under two propagation variants: the vanilla AXW update and the rescaled $AX(2W)$, inspired
 128 by Roth & Liebig (2024, Figure 1). We measure OSM with 2 different metrics: Dirichlet Energy
 129 (DE) and its norm-normalized version, the Rayleigh Coefficient (RQ), which was also previously
 130 used in some works Cai & Wang (2020); Di Giovanni et al. (2023b); Roth & Liebig (2024); Maskey
 131 et al. (2023). Figure 1 shows three key facts: (i) some architectures never collapse, (ii) a minor
 132 rescaling can reverse the trend, and (iii) DE and RQ often disagree. Hence OSM is neither universal
 133 nor straightforward to diagnose.

134 First, OSM, as measured by Dirichlet Energy (DE), is not universal: GIN’s DE explodes instead of
 135 collapsing in the vanilla setting (a), which shows that changing the aggregation-function may lead to
 136 an opposite behavior of OSM effect.

137 Second, a minor scaling in the feature transformation ($2W$ instead of W) flips the behavior of several
 138 models: curves that decayed in (a) now grow or stabilize, and vice-versa. Similar small tweaks
 139 (normalization layers, self-loops, alternative aggregators) can likewise create or remove DE collapse,
 140 which has been leveraged by prior work to propose OSM mitigation approaches, such as the ones
 141 based on feature normalization (Wu et al., 2019; Zhao & Akoglu, 2020; Zhou et al., 2020).

142 Finally, whether OSM is observed depends on the measure of choice. DE reflects raw smoothness,
 143 whereas the RQ normalizes by the feature norm. As a result, the same model can exhibit mutually
 144 contradictory trends for different metrics Zhang et al. (2025). First, GCN’s DE collapses under
 145 the vanilla aggregation (a), explodes with a simple rescaling (b), yet RQ remains essentially flat in
 146 both normalized plots (c-d), indicating that GCN embeddings are being rescaled, not necessarily
 147 oversmoothed. On the contrary, GAT and SAGE, which had similar behavior as GCN in (a) and
 148 (b), decay using RQ (c-d) at a (roughly) linear rate, highlighting how different architectures respond
 149 differently to the use of RQ instead of DE. Furthermore, subfigure (d) shows that $AX(2W)$ can
 150 stabilize RQ for certain methods, suggesting that normalizations or small parameter adjustments do
 151 not affect all models uniformly. Therefore, conclusions about OSM depend heavily on metric and
 152 model, an observation that we rarely found in the literature.

153 In conclusion, OSM is neither inevitable nor uniquely defined: its observation hinges on the archi-
 154 tecture, on seemingly innocuous hyper-parameters, and on which stability metric (DE vs. RQ) one
 155 adopts (Zhang et al., 2022). Therefore, a natural question arises: does OSM actually limit the models’
 156 predictive accuracy? We investigate this question in the next section.

157

158 2.2 BELIEF: OSM IS THE CAUSE OF PERFORMANCE DEGRADATION.

159

160 Part of the literature focuses on the narrative that OSM is the cause of lower test accuracy in DGNs.
 161 The hypothesis is that if embeddings collapse to a non-meaningful space, then the separability of the
 nodes will become challenging and accuracy decreases.

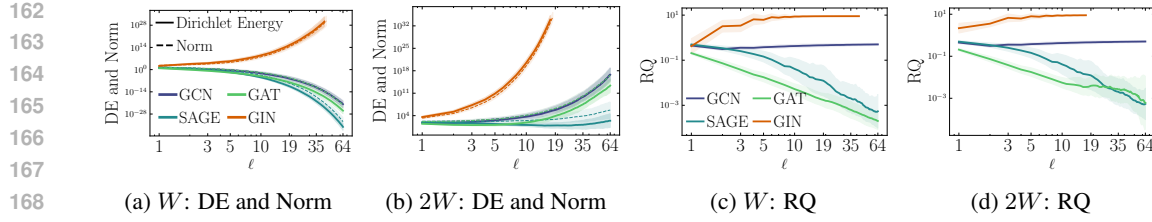


Figure 1: **(a-b)**: We depict the evolution, with increasing number of layers, of the $DE = \text{tr}(X^T \Delta X)$ and the feature norm $\|X\|_F^2$, using W and $2W$ feature transformations for different architectures. **(c-d)**: Evolution of the $RQ = \text{tr}(X^T \Delta X)/\|X\|_F^2$ for W and $2W$ as before. Experiments run on the Cora dataset for 50 random seeds. A larger version for better visualization is available in Fig. 8.

However, this hypothesis ignores some critical aspects, such as *i*) the separability of node embeddings with respect to the nodes' labels, and *ii*) how such separability evolves in the intermediate OSM phase (*if* it happens, as we discussed before).

Regarding the first statement, although it is true that if there is total collapse to the same value then the embeddings will not be informative at all, the main problem remains the node embeddings' separability. As shown in the previous section, some changes in the architectures can avoid OSM, but they might have no impact on the overall accuracy. For instance, multiplying by two the weight matrix leads to a general increase in DE for all architectures, however, the accuracy will remain the same since the embeddings have been simply scaled up and the embeddings' separability is not affected negatively. In addition, avoiding an embedding collapse does not necessarily lead to an improvement in generalization accuracy. For instance, comparing a GCN with and without bias, both versions show a decrease in performance as the number of layers increases, whereas only GCN shows a collapse in DE (Rusch et al., 2023, Figure 3).

On the other hand, and related to the second statement, embedding collapse will not always lead to a decrease in accuracy. OSM happens faster in some subspaces than in others and this effect will be beneficial if labels are correlated with those subspaces Keriven (2022). For instance, if we classify points into two classes, and all nodes of distinct classes collapse into different points, the OSM metric will detect such collapse. However, the separability of the node embeddings will remain possible, illustrating also the limits of wide-spread used OSM metrics with respect to label information.

This intuitive behavior has been identified in the literature as a form of “beneficial” smoothing phase (Keriven, 2022; Roth & Liebig, 2024; Wu et al., 2023b)). In this phase, the nodes of each class first collapse into a class-dependent point before the *potential* second stage, at which point all nodes converge to the same representation. Finally, although overall pairwise distances might shrink in deep layers, *within-class* distances might contract more than *between-class* ones, so class separability improves despite the global collapse, as discussed by Cong et al. (2021).

In conclusion, low accuracy in DGNs cannot be attributed to OSM alone. The separability of node embeddings plays a major role, where other training problems such as vanishing gradients or overfitting also arise when using a big number of layers (Zhao & Akoglu, 2020; Cong et al., 2021; Yang et al., 2020; Arroyo et al., 2025; Park et al., 2025).

Message of the Section

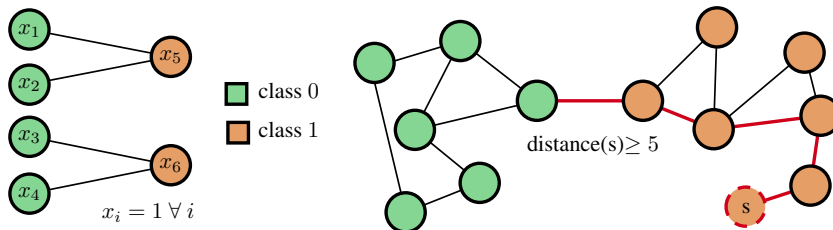
- i) OSM is not a property of all DGNs
- ii) OSM is not necessarily the cause of performance degradation. The performance is related to node embeddings' separability, which can be also affected by many other elements, such as vanishing gradients.
- iii) Therefore, to study the performance of DGNs, it might be better to study how they achieve separability of node embeddings, and how the OSM relates to node separability.

216 3 HOMOPHILY-HETEROGRAPHY AND THE ROLE OF THE TASK

218 In the context of node classification, the term *homophily* (resp. *heterophily*) generally refers to some
 219 form of similarity (resp. dissimilarity) between a node and its neighbors (McPherson et al., 2001).
 220 This (dis)similarity can be measured with respect to class labels, node features, or both; the vast
 221 majority of works in the literature opt for the first, *but this choice is often implicit and taken for*
 222 *granted*, making some statements hard to interpret when one is aware of the other ways to measure it.
 223

224 3.1 BELIEF: HOMOPHILY IS GOOD, HETEROGRAPHY IS BAD

226 A recurrent narrative in the literature is that the message-passing mechanism of DGNs is particularly
 227 suited for homophilic graphs, whereas it is unfit for heterophilic graphs. The apparent motivation is
 228 that, in homophilic graphs, all you need to do to solve a node classification task is to look at similar
 229 neighbors, and a local message-passing strategy implements just the right inductive bias. This is
 230 in contrast to a class-heterophilic graph, where there exist neighboring nodes of a different class
 231 that might make it harder for message-passing to isolate the “relevant information”, intended as
 232 neighbors of the same class. Such a belief is supported by empirical evidence on a rather restricted
 233 set of benchmarks Sen et al. (2008); Namata et al. (2012); Pei et al. (2020) with varying levels of
 234 homophily/heterophily.
 235



243 Figure 2: *Left*: a fully heterophilic graph inspired by (Ma et al., 2022) where a 1-layer, sum-based
 244 DGN can perfectly classify the nodes due to a difference in the node degree. *Right*: a highly
 245 homophilic graph where the task is to predict if a node is at a distance greater than five from a specific
 246 node s . Here, the performances of a DGN will be poor unless information from nodes of another
 247 community – from the perspective of a class-0 node – is captured.
 248

249 Researchers already tried to challenge these considerations in the past Ma et al. (2022); Errica (2023);
 250 Luan et al. (2023); Platonov et al. (2023b); Wang et al. (2024). Consider Figure 2 (left), where a
 251 bipartite graph with identical node features is fully class-heterophilic. If we apply a single sum-based
 252 graph convolution, the nodes can be perfectly classified as the resulting embeddings depend on the
 253 incoming degree. Therefore, **there exist heterophilic graphs where a DGN can achieve perfect**
 254 **classification**. On the contrary, Figure 2 (right) depicts a highly class-homophilic graph, where nodes
 255 belong to one of two classes if they are at a distance greater or lower than five from a given node
 256 s . In this case, the information on the nodes does not even matter; if we were to follow the above
 257 belief, we would be encouraged to use a few layers of message-passing, and as a result **we could**
 258 **never solve the task perfectly**.
 259

260 3.2 BELIEF: DIFFERENT CLASSES IMPLY DIFFERENT FEATURES

261 In the previous section, we deliberately ignored the interplay between a node’s features and its class
 262 label, which is induced by the task at hand. The reason is that we wanted to clarify the distinction
 263 with another, more subtle, and problematic belief: nodes belonging from different classes should
 264 have different (to be read as separable) feature distributions. Under this assumption, it is also implicit
 265 that class homophily will imply feature homophily.
 266

267 Such an assumption is often key in arguments supporting the belief of Section 3.1. Indeed, if nodes of
 268 different classes have different feature distributions, then applying a local message-passing iteration to
 269 a highly class-homophilic graph should “preserve the distance” between node embeddings of different
 270 classes. On the contrary, in a heterophilic setting, a graph convolution would mix information coming
 271 from different feature distributions, which may be detrimental to performances.
 272

270 The logic is not incorrect per-se, but our key counterargument is the following: if different classes
 271 imply different feature distributions, why would one need to apply a DGN rather than a simple MLP?
 272 In other words, **either there is a very strong assumption** that the task does not depend on the
 273 topological information, or the feature-class distributions induced by the task allow us to somehow
 274 take a shortcut in terms of learned function, neglecting the role that the topology might have. Note
 275 that this discussion is irrespective of the denoising/regularizing effects of DGNs in semi-supervised
 276 scenarios compared to MLPs Hoang et al. (2021); Errica (2023).

277 It appears therefore necessary to consider less trivial and more fine-grained scenarios, where the
 278 feature distributions of different classes partially or totally overlap, the topology has a key role in the
 279 task definition, and topological properties induce a positive/negative effect on the performance of
 280 message-passing models as done, for instance, in recent works (Castellana & Errica, 2023; Zheng
 281 et al., 2024).

283 3.3 BELIEF: LONG-RANGE PROPAGATION IS EVALUATED ON HETEROGRAPHIC GRAPHS

285 The common beliefs of Sections 3.1 and 3.2 have been used to support yet another argument, namely
 286 that we should evaluate the ability of DGNs to propagate long-range information on heterophilic
 287 graphs. The rationale seems to be that, in order for DGNs to perform well, nodes of a given class
 288 should focus on information of similar (w.r.t. class and/or features) nodes; therefore, in a heterophilic
 289 graph, it may be necessary to capture information far away (i.e., long-range) from the immediate
 290 neighborhood.

291 Once more, what is really important is to **distinguish the task**, e.g., one that depends on long-range
 292 propagation, **from the class labels the task induces on the nodes**. As a matter of fact, the “long-
 293 range” task of Figure 2 (right) induces a highly homophilic graph, while the heterophilic graph of
 294 Figure 2 (left) is not associated with a long-range propagation task. Therefore, we cannot draw a
 295 generic relation between long-range tasks and heterophily without making further assumptions.

296 Message of the Section

- 298 i) Generic claims about the performance of DGNs under homophily and heterophily do
 299 not hold, nor does their relation with long-range problems.
- 300 ii) Homophily/heterophily is a function of the task, but the converse is not true.
- 301 iii) We should move past the coarse homophily-heterophily dichotomy and **focus more on**
 302 **the task** and the interplay it induces between features, structure, and class labels.

305 4 THE MANY FACETS OF “OVERSQUASHING” AND THEIR NEGATIVE 306 IMPLICATIONS

308 The term oversquashing originated from Alon & Yahav (2021) and referred to an “*exponentially*
 309 *growing information into fixed-size vector*” by repeated application of message-passing. In other
 310 words, oversquashing was associated with the **computational tree** (Figure 3) induced by message-
 311 passing layers on each node of the graph. Later, oversquashing was connected by Topping et al.
 312 (2022) to the existence of **topological bottlenecks**: “*edges with high negative curvature are those*
 313 *causing the graph bottleneck and thus leading to the over-squashing phenomenon*”. Since then,
 314 researchers have adopted one or even both definitions of oversquashing at the same time, contributing
 315 to an apparent understanding that these definitions subsume the same problem.

316 In this section, we argue that **this is not the case** and that, as a community, **we should clearly**
 317 **separate the term “oversquashing”** into (at least) two separate terms:

319 Computational Bottlenecks and Topological Bottlenecks

321 Computational bottlenecks, defined in Def. 4.1, are inevitably related to the *message-passing*
 322 *architecture*, for which the graph is the computational medium, whereas topological bottlenecks
 323 refer to the *graph connectivity*, **usually measured with spectral or curvature metrics defined in**
 B.3.2. **Therefore, the topological bottlenecks are intrinsic to the graph, while the computational**

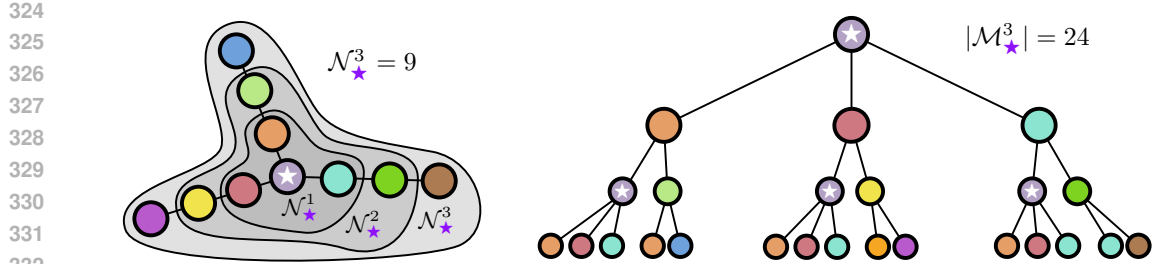


Figure 3: We intuitively visualize what happens when we repeatedly aggregate the neighborhood of the star node using the message-passing paradigm, **where we define the computational bottleneck as the size of the computational tree (24 computational nodes) for $k = 3$ vs the receptive field for $k = 3$ that includes 9 three-hop neighbors**.

bottleneck is intrinsic to the architecture or procedure. While these bottlenecks are clearly intertwined, in the following we show that they do not always coexist, hence it makes sense to treat them as **fundamentally distinct concepts**.

Computational and Topological Bottleneck definitions. Although both bottlenecks have been previously used to measure “*oversquashing*”, their definitions and measurement approaches also differ across the literature. There is no universally accepted formal definition of a *topological* bottleneck; instead, it is typically characterized using proxy metrics, most often involving the spectral gap of the curvature. Some of the most significant metrics are summarized in B.3.2.

On the other hand, the *computational* bottleneck has been usually measured using the *receptive field* (Chen et al., 2018; Alon & Yahav, 2021), \mathcal{N}_v^k , as the set of K -hop neighbors neighbors, which grows exponentially with the number of layers.

However, when evaluating the actual *computational* graph produced by message-passing, shown in Figure 3 (right), duplicate nodes become significant: a node appearing in multiple branches of the computation tree contributes repeatedly, as each unique walk generates a distinct message. Consequently, we employ multiset notation to formally define the *computational tree* for a node v :

$$\mathcal{M}_v^1 := \mathcal{N}_v, \quad \mathcal{M}_v^K := \mathcal{M}_v^{K-1} \uplus \left\{ \biguplus_{u \in \mathcal{M}_v^{K-1}} \mathcal{N}_u \right\}. \quad (2)$$

Therefore, we can define the notion of an “exponentially-growing receptive field” Alon & Yahav (2021) as follows:

Definition 4.1 (Computational Bottleneck). For a given node v and number of message passing layers K , the computational bottleneck of node v is defined as $|\mathcal{M}_v^K|$.

We refer the reader to B.4 for further insights, related work, and connections between this definition and matrix-power interpretations of message passing.

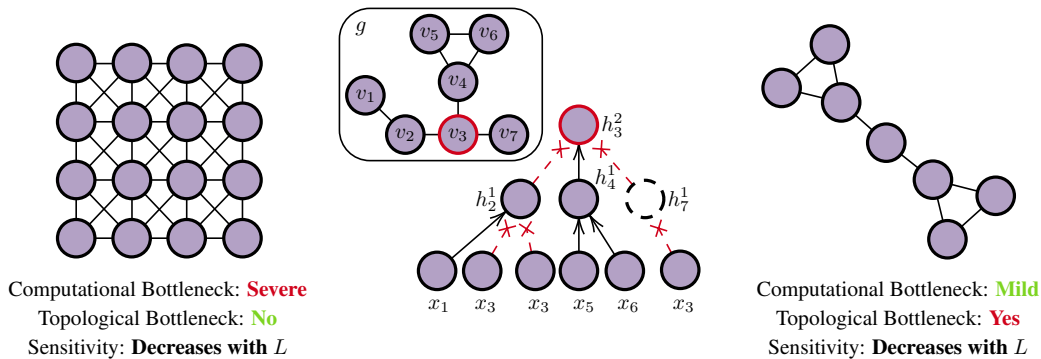
Figure 3 visualises the difference between the set size $|\mathcal{N}_v^K|$ and the multiset size $|\mathcal{M}_v^K|$ on a toy graph and on a stochastic block model (SBM).

4.1 BELIEF: OVERSQUASHING AS SYNONYM OF TOPOLOGICAL BOTTLENECK

The prolific line of work that associates “oversquashing” with topological bottlenecks seems to have gained popularity with Topping et al. (2022). In that paper, edges with negative curvature are first associated with (topological) bottlenecks, then a theorem puts in relation message-passing on a graph containing a bottleneck with the Jacobian sensitivity of node representations, typically defined by $I(u, v) = \|\partial \mathbf{h}_u^K / \partial \mathbf{h}_v^0\|$ and denoting how much the final representation of a node u after K layers is influenced by the initial representation of a node v (Xu et al., 2018). Put simply, a

378 topological bottleneck may imply low sensitivity. **However, the converse is not necessarily true:**
 379 we can have low sensitivity on a graph where there are no bottlenecks. Figure 4 (left) shows a grid
 380 graph where there are no topological bottlenecks. The repeated application of message passing will,
 381 however, quickly generate a computational bottleneck. Therefore, saying that there are no topological
 382 bottlenecks does not imply that there are no computational bottlenecks.

383 To improve on topological bottlenecks, a widely investigated approach is graph rewiring (Attali et al.,
 384 2024b), which was also the subject of scrutiny recently (Tortorella & Micheli, 2022; Tori et al., 2025).
 385 Rewiring is based on the intuition that improving topological bottlenecks metrics should improve
 386 the performance of DGNs (Arnaiz-Rodriguez et al., 2022; Banerjee et al., 2022; Karhadkar et al.,
 387 2023; Deac et al., 2022), by reducing the distance between nodes that should communicate. At the
 388 same time, it should become clear now that, under the DGN paradigm, *rewiring might worsen the*
 389 *computational bottleneck* – as long as the same number of message-passing layers is used – while
 390 improving the topological one. This perspective was also put forward by Errica et al. (2025), with
 391 a theoretical analysis on how message filtering,³ as shown in Figure 4 (middle), reduces both the
 392 computational bottleneck and sensitivity yet improves performances while leaving the graph structure
 393 unaltered.



403 Figure 4: *Left*: in a grid graph, the computational bottleneck grows very quickly but there is no
 404 topological bottleneck. *Middle*: A visualization of the computational graph rooted at node $v_3 \in \mathcal{V}_g$
 405 for two message passing layers, highlighting how pruning messages reduces the computational
 406 bottleneck. *Right*: In this graph, there is a topological bottleneck and a mild computational bottleneck.
 407 As with the grid graph (Appendix C), the sensitivity decreases with the number of message-passing
 408 layers.

409 Another, slightly more technical way to see why low Jacobian sensitivity does not imply the presence
 410 of any topological bottlenecks is to follow the chain of upper bounds that link the metrics used to
 411 measure the computational and topological bottlenecks (Black et al., 2023; Di Giovanni et al., 2023b;
 412 Karhadkar et al., 2023; Arnaiz-Rodriguez et al., 2022). Several recent works (Black et al., 2023;
 413 Di Giovanni et al., 2023a) have shown that sensitivity is bounded by above by a term that includes
 414 the effective resistance, a purely topological distance metric that quantifies the expected commute
 415 time of a random walk between nodes u and v (Klein & Randić, 1993). In particular, the bound
 416 subtracts the lower bound on the maximum effective resistance, which depends on the inverse of
 417 the spectral gap (a proxy for topological bottlenecks) (Chandra et al., 1989; Lovász, 1993). This
 418 connection provides a useful intuition: as the topological bottleneck gets worse, the lower bound on
 419 the maximum effective resistance increases, which in turn reduces the upper bounds on the sensitivity
 420 of Black et al. (2023). **However, the converse does not hold.** There are graphs where the maximum
 421 effective resistance between distant nodes is large despite the absence of topological bottlenecks.
 422 For instance, consider the example of a grid graph in Figure 4 (left) where there is no topological
 423 bottleneck, yet the effective resistance between diagonally opposite corners grows linearly with the
 424 grid size. As a result, sensitivity between those nodes decays with depth, even though the graph
 425 has no identifiable topological bottlenecks. This illustrates that computational bottlenecks can arise

426
 427
 428
 429
 430
 431 ³The concept of *message filtering* refers to message passing architectures with the ability to learn how many
 432 messages to exchange between nodes and which messages to filter out.

432 independently of topological ones, **and that low sensitivity does not necessarily imply the presence**
 433 **of either of them.**

435 4.2 BELIEF: OVERSQUASHING AS SYNONYM OF COMPUTATIONAL BOTTLENECK

437 We briefly complement the previous section with a discussion on “oversquashing” as a computational
 438 bottleneck, which was introduced by Alon & Yahav (2021) and has been the (often implicit) study
 439 subject of works that prune, to some extent, the computational tree induced on every node by the
 440 iterative message-passing process (Rong et al., 2020; Erica et al., 2025). Also in this case, there
 441 exist cases where reducing the computational bottleneck may be harmful: Figure 4 (right) shows a
 442 graph where there is a topological bottleneck but no severe computational bottleneck (for a limited
 443 number of layers). In this case, excessive pruning of the computational tree might cause distant nodes
 444 to interrupt all communications. Therefore, computational and topological bottlenecks are problems
 445 that should be tackled separately.

446 4.3 BELIEF: OVERSQUASHING IS PROBLEMATIC FOR LONG-RANGE TASKS

448 Since its definition by Alon & Yahav (2021), oversquashing has often been considered a problem
 449 in long-range tasks. The reason stems from its relation to the exponentially growing computa-
 450 tional tree as the number of message-passing layers increases: whenever a node has to receive
 451 information from another node at distance d , classical (synchronous) message-passing architectures
 452 need to apply at least d layers to capture that information. As a result, the relevant information
 453 may get lost due to the exponentially large computational bottleneck.
 454 Importantly, topological bottlenecks can only make the problem
 455 worse, by forcing the information of a group of messages to be
 456 squeezed through an edge – please refer to the next section for a
 457 discussion about long-range tasks and topological bottlenecks.

458 The main message here is that long-range tasks “force” classical
 459 message-passing architecture to create a computational bottleneck
 460 to propagate the necessary information, **but one can observe com-**
461 putational bottlenecks even in short-range tasks. An obvious
 462 example is the high-degree node of Figure 5, where, after *just one*
 463 layer, the center node receives a high number of messages, effec-
 464 tively creating a computational bottleneck in terms of information
 465 to be squashed into a fixed-size vector. Therefore, while the task of
 466 long-range is related to computational bottlenecks under classical
 467 DGNs, computational bottlenecks are not a prerogative of long-range tasks.

468 4.4 BELIEF: TOPOLOGICAL BOTTLENECKS ASSOCIATED WITH LONG-RANGE PROBLEMS

470 The last belief we discuss is that topological bottlenecks are the primary obstacle to solving long-
 471 range tasks. This intuition stems from the fact that narrow cuts impede information flow between
 472 distant parts of the graph. It is indeed true that a topological bottleneck can worsen communication
 473 between distant nodes, especially if the bottleneck lies along a path that connects them. However, this
 474 perspective is limited in two important ways. First, a topological bottleneck is only harmful if it lies
 475 on the information paths between nodes that are supposed to communicate. A topological bottleneck
 476 may exist without affecting task-relevant dependencies. Second, the graph topology can worsen the
 477 long-range communication even in the absence of any identifiable topological bottleneck, by inducing
 478 computational bottlenecks. As we discussed in Section 4.1, the grid graph is an illustrative case:
 479 despite the lack of topological bottlenecks, to connect the opposite corner nodes we need, at least, as
 480 many message-passing layers as the distance between them, thus leading to a huge computational
 481 bottleneck that will likely hamper the ability to process long-range dependencies.

482 In addition, some of the techniques that reduce topological bottlenecks rely on introducing more
 483 edges or nodes into the graph, with the aim of reducing the distance between far-away nodes that
 484 should communicate. It is important to note that, although these approaches might be beneficial
 485 for the task at hand, they also worsen the computational bottleneck by adding more branches to the
 computational tree.

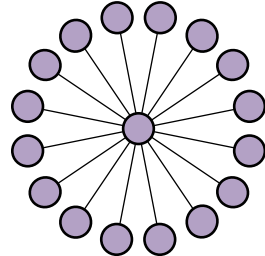


Figure 5: Hubs can exhibit computational bottlenecks.

486 In conclusion, this highlights a deeper issue: long-range problems are not solely caused by topo-
 487 logical bottlenecks, rather they can be understood as a form of information attenuation caused by
 488 computational bottlenecks in the message-passing mechanism, which can potentially be exacerbated
 489 by topological bottlenecks. Thus, solving a topological bottleneck is neither necessary nor sufficient
 490 to solve all long-range problems.

491 Message of the Section

- 493 i) “Oversquashing” is an ambiguous term that led to unclear research statements. Talking
 494 about **computational and topological bottlenecks**, instead, better defines the research
 495 scope of a paper, since **they are two fundamentally distinct problems**.
- 496 ii) There can be computational bottlenecks but no topological ones, and vice-versa. Hence,
 497 each of these two bottlenecks, though intertwined, deserves a dedicated research effort.
 498 This also means **creating ad-hoc benchmarks for each type of bottleneck rather than**
 499 **relying solely on real-world tasks**, where it is not as easy to distinguish the combined
 500 effect of the two bottlenecks.
- 501 iii) Computational bottlenecks can happen in short-range as well as long-range tasks.
- 502 iv) Performance issues in long-range tasks are not solely caused by topological bottlenecks;
 503 computational bottlenecks play a role as well.

505 5 CONCLUSIONS

506 This paper posits that the fast pace of advances in the graph machine learning field has generated
 507 several commonly accepted beliefs and hypotheses, rooted in the notions of oversmoothing, “over-
 508 squashing”, long-range tasks, and heterophily, which are the cause of misunderstandings between
 509 researchers. Our contribution was to highlight such beliefs in plain sight, provide an explanation
 510 for their emergence, and demystify them when necessary with simple counterexamples. First, we
 511 argued that OSM may not be an actual problem and that node embeddings’ separability should be
 512 preferred when looking for the root causes of performance degradation. Then, we showed how
 513 talking about computational and topological bottlenecks resolves most, if not all, inconsistencies
 514 generated by the inflated use of the “oversquashing” term. Finally, we highlighted the role of the
 515 task in statements involving homophily, heterophily, and long-range dependencies. By providing
 516 much-needed clarifications around these aspects, we hope to foster further advancements in the graph
 517 machine learning field.

521 REFERENCES

523 Ralph Abboud, Radoslav Dimitrov, and Ismail Ilkan Ceylan. Shortest path networks for graph
 524 property prediction. In *The 1st Learning on Graphs Conference (LoG)*, 2022.

525 Sami Abu-El-Haija, Bryan Perozzi, Amol Kapoor, Nazanin Alipourfard, Kristina Lerman, Hrayr
 526 Harutyunyan, Greg Ver Steeg, and Aram Galstyan. Mixhop: Higher-order graph convolutional
 527 architectures via sparsified neighborhood mixing. In *Proceedings of the 36th International
 528 Conference on Machine Learning (ICML)*, 2019.

530 Singh Akansha. Over-squashing in graph neural networks: A comprehensive survey. *arXiv preprint
 531 arXiv:2308.15568*, 2023.

532 Uri Alon and Eran Yahav. On the bottleneck of graph neural networks and its practical implications.
 533 In *Proceedings of the 9th International Conference on Learning Representations (ICLR)*, 2021.

535 Adrian Arnaiz-Rodriguez and Ameya Velingker. Graph Learning: Principles, Challenges, and Open
 536 Directions. In *41st International Conference on Machine Learning (ICML)*, 2024. Tutorial.

538 Adrian Arnaiz-Rodriguez, Ahmed Begga, Francisco Escolano, and Nuria M Oliver. DiffWire:
 539 Inductive Graph Rewiring via the Lovász Bound. In *Proceedings of the 1st Learning on Graphs
 Conference (LoG)*, 2022.

540 Álvaro Arroyo, Alessio Gravina, Benjamin Gutteridge, Federico Barbero, Claudio Gallicchio,
 541 Xiaowen Dong, Michael Bronstein, and Pierre Vandergheynst. On vanishing gradients, over-
 542 smoothing, and over-squashing in gnn: Bridging recurrent and graph learning. *arXiv preprint*
 543 *arXiv:2502.10818*, 2025.

544 Hugo Attali, Davide Buscaldi, and Nathalie Pernelle. Delaunay graph: Addressing over-squashing and
 545 over-smoothing using delaunay triangulation. In *Proceedings of the 41st International Conference*
 546 *on Machine Learning (ICML)*, 2024a.

547 Hugo Attali, Davide Buscaldi, and Nathalie Pernelle. Rewiring techniques to mitigate oversquashing
 548 and oversmoothing in gnn: A survey. *arXiv preprint arXiv:2411.17429*, 2024b.

549 Davide Baci, Federico Errica, Alessio Michel, and Marco Podda. A gentle introduction to deep
 550 learning for graphs. *Neural Networks*, 129, 2020.

551 Julia Balla. Over-squashing in riemannian graph neural networks. In *Proceedings of the 2nd Learning*
 552 *on Graphs Conference (LoG)*, 2023.

553 Pradeep Kr Banerjee, Kedar Karhadkar, Yu Guang Wang, Uri Alon, and Guido Montúfar. Over-
 554 squashing in gnn through the lens of information contraction and graph expansion. In *Proceedings*
 555 *of the 58th Annual Allerton Conference on Communication, Control, and Computing (Allerton)*,
 556 2022.

557 Federico Barbero, Ameya Velingker, Amin Saberi, Michael M. Bronstein, and Francesco Di Giovanni.
 558 Locality-aware graph rewiring in GNNs. In *Proceedings of the 12th International Conference on*
 559 *Learning Representations (ICLR)*, 2024.

560 Dominique Beaini, Shenyang Huang, Joao Alex Cunha, Zhiyi Li, Gabriela Moisescu-Pareja,
 561 Oleksandr Dymov, Samuel Maddrell-Mander, Callum McLean, Frederik Wenkel, Luis Müller,
 562 Jama Hussein Mohamud, Ali Parviz, Michael Craig, Michał Koziarski, Jiarui Lu, Zhaocheng
 563 Zhu, Cristian Gabellini, Kerstin Klaser, Josef Dean, Cas Wognum, Maciej Sypetkowski, Guil-
 564 laume Rabusseau, Reihaneh Rabbany, Jian Tang, Christopher Morris, Mirco Ravanelli, Guy Wolf,
 565 Prudencio Tossou, Hadrien Mary, Thérènce Bois, Andrew W Fitzgibbon, Blazej Banaszewski,
 566 Chad Martin, and Dominic Masters. Towards foundational models for molecular learning on
 567 large-scale multi-task datasets. In *Proceedings of the 12th International Conference on Learning*
 568 *Representations (ICLR)*, 2024.

569 Wendong Bi, Lun Du, Qiang Fu, Yanlin Wang, Shi Han, and Dongmei Zhang. Make heterophilic
 570 graphs better fit gnn: A graph rewiring approach. *IEEE Transactions on Knowledge and Data*
 571 *Engineering*, 2024.

572 Mitchell Black, Zhengchao Wan, Amir Nayyeri, and Yusu Wang. Understanding oversquashing in
 573 gnn through the lens of effective resistance. In *Proceedings of the 40th International Conference*
 574 *on Machine Learning (ICML)*, 2023.

575 Cristian Bodnar, Francesco Di Giovanni, Benjamin Chamberlain, Pietro Lio, and Michael Bronstein.
 576 Neural sheaf diffusion: A topological perspective on heterophily and oversmoothing in gnn.
 577 In *Proceedings of the 36th Conference on Advances in Neural Information Processing Systems*
 578 (*NeurIPS*), 2022.

579 Chen Cai and Yusu Wang. A note on over-smoothing for graph neural networks. In *Graph Repre-
 580 sentation Learning and Beyond Workshop, 37th International Conference on Machine Learning*
 581 (*ICML*), 2020.

582 Chen Cai, Truong Son Hy, Rose Yu, and Yusu Wang. On the connection between mpnn and graph
 583 transformer. In *Proceedings of the 40th International Conference on Machine Learning (ICML)*,
 584 pp. 3408–3430, 2023.

585 Daniele Castellana and Federico Errica. Investigating the interplay between features and structures in
 586 graph learning. In *MLG Workshop at ECML PKDD*, 2023.

587 Ashok K Chandra, Prabhakar Raghavan, Walter L Ruzzo, and Roman Smolensky. The electrical
 588 resistance of a graph captures its commute and cover times. In *Proceedings of the twenty-first*
 589 *annual ACM symposium on Theory of computing*, pp. 574–586, 1989.

594 Deli Chen, Yankai Lin, Wei Li, Peng Li, Jie Zhou, and Xu Sun. Measuring and relieving the over-
 595 smoothing problem for graph neural networks from the topological view. In *Proceedings of the*
 596 *34th AAAI conference on artificial intelligence (AAAI)*, 2020a.

597 Jianfei Chen, Jun Zhu, and Le Song. Stochastic training of graph convolutional networks with
 598 variance reduction. In *Proceedings of the 35th International Conference on Machine Learning*
 599 (*ICML*), 2018.

600 Ming Chen, Zhewei Wei, Zengfeng Huang, Bolin Ding, and Yaliang Li. Simple and deep graph
 601 convolutional networks. In *Proceedings of the 37th International Conference on Machine Learning*
 602 (*ICML*), 2020b.

603 Tianlong Chen, Kaixiong Zhou, Keyu Duan, Wenqing Zheng, Peihao Wang, Xia Hu, and Zhangyang
 604 Wang. Bag of tricks for training deeper graph neural networks: A comprehensive benchmark study.
 605 *IEEE Transactions on Pattern Analysis and Machine Intelligence*, 45(3), 2022.

606 Fan RK Chung. *Spectral graph theory*, volume 92. American Mathematical Soc., 1997.

607 Weilin Cong, Morteza Ramezani, and Mehrdad Mahdavi. On provable benefits of depth in training
 608 graph convolutional networks. *Advances in Neural Information Processing Systems*, 34:9936–9949,
 609 2021.

610 Andreea Deac, Marc Lackenby, and Petar Veličković. Expander graph propagation. In *Proceedings*
 611 *of the 1st Learning on Graphs Conference (LoG)*, 2022.

612 Francesco Di Giovanni, Lorenzo Giusti, Federico Barbero, Giulia Luise, Pietro Lio, and Michael M
 613 Bronstein. On over-squashing in message passing neural networks: The impact of width, depth,
 614 and topology. In *Proceedings of the 40th International Conference on Machine Learning (ICML)*,
 615 2023a.

616 Francesco Di Giovanni, James Rowbottom, Benjamin Paul Chamberlain, Thomas Markovich, and
 617 Michael M. Bronstein. Understanding convolution on graphs via energies. *Transactions on*
 618 *Machine Learning Research*, 2023b.

619 Francesco Di Giovanni, T. Konstantin Rusch, Michael Bronstein, Andreea Deac, Marc Lackenby,
 620 Siddhartha Mishra, and Petar Veličković. How does over-squashing affect the power of GNNs?
 621 *Transactions on Machine Learning Research*, 2024.

622 Vijay Prakash Dwivedi, Ladislav Rampášek, Michael Galkin, Ali Parviz, Guy Wolf, Anh Tuan Luu,
 623 and Dominique Beaini. Long range graph benchmark. In *Proceedings of the 36th Conference on*
 624 *Neural Information Processing Systems (NeurIPS)*, 2022.

625 Wendy Ellens, Floske M Spieksma, Piet Van Mieghem, Almerima Jamakovic, and Robert E Kooij.
 626 Effective graph resistance. *Linear algebra and its applications*, 435(10):2491–2506, 2011.

627 Bastian Epping, Alexandre René, Moritz Helias, and Michael T Schaub. Graph neural networks do
 628 not always oversmooth. In *Proceedings of the 38th Conference on Neural Information Processing*
 629 *Systems (NeurIPS)*, 2024.

630 Federico Errica. On class distributions induced by nearest neighbor graphs for node classification of
 631 tabular data. In *Proceedings of the 37th Conference on Advances in Neural Information Processing*
 632 *Systems (NeurIPS)*, 2023.

633 Federico Errica, Henrik Christiansen, Viktor Zaverkin, Takashi Maruyama, Mathias Niepert, and
 634 Francesco Alesiani. Adaptive message passing: A general framework to mitigate oversmoothing,
 635 oversquashing, and underreaching. In *Proceedings of the 42nd International Conference on*
 636 *Machine Learning (ICML)*, 2025.

637 Lukas Fesser and Melanie Weber. Mitigating over-smoothing and over-squashing using augmentations
 638 of forman-ricci curvature. In *Proceedings of the 4th Learning on Graphs Conference (LoG)*, 2024.

639 Rickard Brüel Gabrielsson, Mikhail Yurochkin, and Justin Solomon. Rewiring with positional
 640 encodings for graph neural networks. *Transactions on Machine Learning Research*, 2023.

648 Johannes Gasteiger, Aleksandar Bojchevski, and Stephan Günnemann. Predict then propagate: Graph
 649 neural networks meet personalized pagerank. In *Proceedings of the 7th International Conference*
 650 *on Learning Representations (ICLR)*, 2019.

651

652 Justin Gilmer, Samuel S Schoenholz, Patrick F Riley, Oriol Vinyals, and George E Dahl. Neural
 653 message passing for quantum chemistry. In *Proceedings of the 34th International Conference on*
 654 *Machine Learning (ICML)*, 2017.

655 Jhony H Giraldo, Konstantinos Skianis, Thierry Bouwmans, and Fragkiskos D Malliaros. On the trade-
 656 off between over-smoothing and over-squashing in deep graph neural networks. In *Proceedings of*
 657 *the 32nd ACM International Conference on Information and Knowledge Management (ICKM)*,
 658 2023.

659

660 Chenghua Gong, Yao Cheng, Jianxiang Yu, Can Xu, Caihua Shan, Siqiang Luo, and Xiang Li. A
 661 survey on learning from graphs with heterophily: Recent advances and future directions. *arXiv*
 662 preprint *arXiv:2401.09769*, 2024.

663

664 Marco Gori, Gabriele Monfardini, and Franco Scarselli. A new model for learning in graph domains.
 In *Proceedings of the International Joint Conference on Neural Networks (IJCNN)*, 2005.

665

666 Alessio Gravina, Moshe Eliasof, Claudio Gallicchio, Davide Bacciu, and Carola-Bibiane Schönlieb.
 667 On oversquashing in graph neural networks through the lens of dynamical systems. In *Proceedings*
 668 *of the 39th AAAI Conference on Artificial Intelligence (AAAI)*, 2025.

669

670 Benjamin Gutteridge, Xiaowen Dong, Michael M Bronstein, and Francesco Di Giovanni. Drew:
 671 Dynamically rewired message passing with delay. In *Proceedings of the 40th International*
 672 *Conference on Machine Learning (ICML)*, 2023.

673

674 William L Hamilton. *Graph representation learning*. Morgan & Claypool Publishers, 2020.

675

676 Arman Hasanzadeh, Ehsan Hajiramezanali, Shahin Boluki, Mingyuan Zhou, Nick Duffield, Krishna
 677 Narayanan, and Xiaoning Qian. Bayesian graph neural networks with adaptive connection sampling.
 In *Proceedings of the 37th International Conference on Machine Learning (ICML)*, 2020.

678

679 NT Hoang, Takanori Maehara, and Tsuyoshi Murata. Revisiting graph neural networks: Graph
 680 filtering perspective. In *Proceedings of the 25th International Conference on Pattern Recognition*
 681 (*ICPR*), 2021.

682

683 Keke Huang, Yu Guang Wang, Ming Li, and Pietro Lio. How universal polynomial bases enhance
 684 spectral graph neural networks: Heterophily, over-smoothing, and over-squashing. In *Proceedings*
 685 *of the 41st International Conference on Machine Learning (ICML)*, 2024.

686

687 Wenbing Huang, Yu Rong, Tingyang Xu, Fuchun Sun, and Junzhou Huang. Tackling over-smoothing
 688 for general graph convolutional networks. *arXiv preprint arXiv:2008.09864*, 2020.

689

690 EunJeong Hwang, Veronika Thost, Shib Sankar Dasgupta, and Tengfei Ma. An analysis of virtual
 691 nodes in graph neural networks for link prediction (extended abstract). In *Proceedings of the 1st*
 692 *Learning on Graphs Conference (LoG)*, 2022.

693

694 Adarsh Jamadandi, Celia Rubio-Madrigal, and Rebekka Burkholz. Spectral graph pruning against
 695 over-squashing and over-smoothing. In *Proceedings of the 38th Conference on Neural Information*
 696 *Processing Systems (NeurIPS)*, 2024.

697

698 Kedar Karhadkar, Pradeep Kr. Banerjee, and Guido Montufar. FoSR: First-order spectral rewiring
 699 for addressing oversquashing in GNNs. In *Proceedings of the 11th International Conference on*
 700 *Learning Representations (ICLR)*, 2023.

701

Nicolas Keriven. Not too little, not too much: a theoretical analysis of graph (over) smoothing.
 In *Proceedings of the 36th Conference on Advances in Neural Information Processing Systems*
 (NeurIPS), 2022.

Thomas N Kipf and Max Welling. Semi-supervised classification with graph convolutional networks.
 In *Proceedings of the 5th International Conference on Learning Representations (ICLR)*, 2017.

702 Douglas J Klein and Milan Randić. Resistance distance. *Journal of mathematical chemistry*, 12: 703 81–95, 1993.

704

705 Guohao Li, Matthias Muller, Ali Thabet, and Bernard Ghanem. Deepgcns: Can gcns go as deep 706 as cnns? In *Proceedings of the 17th IEEE/CVF International Conference on Computer Vision 707 (ICCV)*, 2019.

708 Qimai Li, Zhichao Han, and Xiao-Ming Wu. Deeper insights into graph convolutional networks for 709 semi-supervised learning. In *Proceedings of the 32nd AAAI conference on artificial intelligence 710 (AAAI)*, 2018.

711 Derek Lim, Felix Hohne, Xiuyu Li, Sijia Linda Huang, Vaishnavi Gupta, Omkar Bhalerao, and 712 Ser Nam Lim. Large scale learning on non-homophilous graphs: New benchmarks and strong 713 simple methods. In *Proceedings of the 35th Conference on Neural Information Processing Systems 714 (NeurIPS)*, 2021.

715

716 Meng Liu, Hongyang Gao, and Shuiwang Ji. Towards deeper graph neural networks. In *Proceedings 717 of the 26th ACM SIGKDD International Conference on Knowledge Discovery & Data Mining 718 (KDD)*, pp. 338–348, 2020.

719 Yang Liu, Chuan Zhou, Shirui Pan, Jia Wu, Zhao Li, Hongyang Chen, and Peng Zhang. Curvdrop: 720 A ricci curvature based approach to prevent graph neural networks from over-smoothing and 721 over-squashing. In *Proceedings of the ACM International World Wide Web Conference (WWW)*, 722 2023a.

723

724 Yixin Liu, Yizhen Zheng, Daokun Zhang, Vincent CS Lee, and Shirui Pan. Beyond smoothing: 725 Unsupervised graph representation learning with edge heterophily discriminating. In *Proceedings 726 of the AAAI Conference on Artificial Intelligence (AAAI)*, 2023b.

727 Antonio Longa, Veronica Lachi, Gabriele Santin, Monica Bianchini, Bruno Lepri, Pietro Lio, franco 728 scarselli, and Andrea Passerini. Graph neural networks for temporal graphs: State of the art, open 729 challenges, and opportunities. *Transactions on Machine Learning Research*, 2023.

730 László Lovász. Random walks on graphs. *Combinatorics, Paul erdos is eighty*, 2(1-46):4, 1993. URL 731 <https://web.cs.elte.hu/~lovasz/erdos.pdf>.

732

733 Sitao Luan, Chenqing Hua, Qincheng Lu, Jiaqi Zhu, Mingde Zhao, Shuyuan Zhang, Xiao-Wen 734 Chang, and Doina Precup. Is heterophily a real nightmare for graph neural networks to do node 735 classification? *arXiv preprint arXiv:2109.05641*, 2021.

736 Sitao Luan, Chenqing Hua, Qincheng Lu, Jiaqi Zhu, Mingde Zhao, Shuyuan Zhang, Xiao-Wen 737 Chang, and Doina Precup. Revisiting heterophily for graph neural networks. In *Proceedings of the 738 36th Conference on Advances in Neural Information Processing Systems (NeurIPS)*, 2022.

739

740 Sitao Luan, Chenqing Hua, Minkai Xu, Qincheng Lu, Jiaqi Zhu, Xiao-Wen Chang, Jie Fu, Jure 741 Leskovec, and Doina Precup. When do graph neural networks help with node classification? 742 investigating the homophily principle on node distinguishability. In *Proceedings of the 37th 743 Conference on Neural Information Processing Systems (NeurIPS)*, 2023.

744 Yao Ma, Xiaorui Liu, Neil Shah, and Jiliang Tang. Is homophily a necessity for graph neural 745 networks? In *10th International Conference on Learning Representations (ICLR)*, 2022.

746

747 Sohir Maskey, Raffaele Paolino, Aras Bacho, and Gitta Kutyniok. A fractional graph laplacian 748 approach to oversmoothing. In *Proceedings of the 37th Conference on Neural Information 749 Processing Systems (NeurIPS)*, 2023.

750 Miller McPherson, Lynn Smith-Lovin, and James M Cook. Birds of a feather: Homophily in social 751 networks. *Annual review of sociology*, 27, 2001.

752 Alessio Micheli. Neural network for graphs: A contextual constructive approach. *IEEE Transactions 753 on Neural Networks*, 20, 2009.

754

755 Alessio Micheli and Antonio Sestito. A new neural network model for contextual processing of 756 graphs. In *Proceedings of the Italian Workshop on Neural Networks (WIRN)*, 2005.

756 Christopher Morris, Yaron Lipman, Haggai Maron, Bastian Rieck, Nils M Kriege, Martin Grohe,
 757 Matthias Fey, and Karsten Borgwardt. Weisfeiler and leman go machine learning: The story so far.
 758 *Journal of Machine Learning Research*, 24, 2023.

759 Galileo Mark Namata, Ben London, Lise Getoor, and Bert Huang. Query-driven active surveying for
 760 collective classification. In *Proceedings of the Workshop on Mining and Learning with Graphs*
 761 (*MLG*), 2012.

762 Khang Nguyen, Nong Minh Hieu, Vinh Duc Nguyen, Nhat Ho, Stanley Osher, and Tan Minh Nguyen.
 763 Revisiting over-smoothing and over-squashing using ollivier-ricci curvature. In *Proceedings of the*
 764 *40th International Conference on Machine Learning (ICML)*, 2023.

765 Kenta Oono and Taiji Suzuki. Graph neural networks exponentially lose expressive power for node
 766 classification. In *Proceedings of the 8th International Conference on Learning Representations*
 767 (*ICLR*), 2020.

768 MoonJeong Park, Sunghyun Choi, Jaeseung Heo, Eunhyeok Park, and Dongwoo Kim. The over-
 769 smoothing fallacy: A misguided narrative in gnn research. *arXiv preprint arXiv:2506.04653*,
 770 2025.

771 Hongbin Pei, Bingzhe Wei, Kevin Chen-Chuan Chang, Yu Lei, and Bo Yang. Geom-gcn: Geometric
 772 graph convolutional networks. In *Proceedings of the 8th International Conference on Learning*
 773 *Representations (ICLR)*, 2020.

774 Oleg Platonov, Denis Kuznedelev, Artem Babenko, and Liudmila Prokhorenkova. Characterizing
 775 graph datasets for node classification: Homophily-heterophily dichotomy and beyond. In
 776 *Proceedings of the 37th Conference on Neural Information Processing Systems (NeurIPS)*, 2023a.

777 Oleg Platonov, Denis Kuznedelev, Michael Diskin, Artem Babenko, and Liudmila Prokhorenkova.
 778 A critical look at the evaluation of GNNs under heterophily: Are we really making progress? In
 779 *Proceedings of the 1th International Conference on Learning Representations (ICLR)*, 2023b.

780 Huaijun Qiu and Edwin R Hancock. Clustering and embedding using commute times. *IEEE*
 781 *Transactions on Pattern Analysis and Machine Intelligence*, 29(11):1873–1890, 2007.

782 Yu Rong, Wenbing Huang, Tingyang Xu, and Junzhou Huang. Dropedge: Towards deep graph
 783 convolutional networks on node classification. In *Proceedings of the 8th International Conference*
 784 *on Learning Representations*, 2020.

785 Andreas Roth and Thomas Liebig. Rank collapse causes over-smoothing and over-correlation in
 786 graph neural networks. In *Proceedings of the 3rd Learning on Graphs Conference (LoG)*, 2024.

787 T Konstantin Rusch, Ben Chamberlain, James Rowbottom, Siddhartha Mishra, and Michael Bronstein.
 788 Graph-coupled oscillator networks. In *Proceedings of the 39th International Conference on*
 789 *Machine Learning (ICML)*, 2022.

790 T Konstantin Rusch, Michael M Bronstein, and Siddhartha Mishra. A survey on oversmoothing in
 791 graph neural networks. *arXiv preprint arXiv:2303.10993*, 2023.

792 Franco Scarselli, Marco Gori, Ah Chung Tsoi, Markus Hagenbuchner, and Gabriele Monfardini. The
 793 graph neural network model. *IEEE Transactions on Neural Networks*, 20, 2009.

794 Prithviraj Sen, Galileo Namata, Mustafa Bilgic, Lise Getoor, Brian Galligher, and Tina Eliassi-Rad.
 795 Collective classification in network data. *AI magazine*, 29(3):93–93, 2008.

796 Zhiqi Shao, Dai Shi, Andi Han, Yi Guo, Qibin Zhao, and Junbin Gao. Unifying over-smoothing
 797 and over-squashing in graph neural networks: A physics informed approach and beyond. *arXiv*
 798 *preprint arXiv:2309.02769*, 2023.

799 Dai Shi, Andi Han, Lequan Lin, Yi Guo, and Junbin Gao. Exposition on over-squashing problem on
 800 gnns: Current methods, benchmarks and challenges. *arXiv preprint arXiv:2311.07073*, 2023.

801 Joshua Southern, Francesco Di Giovanni, Michael Bronstein, and Johannes F Lutzeyer. Under-
 802 standing virtual nodes: Oversmoothing, oversquashing, and node heterogeneity. *arXiv preprint*
 803 *arXiv:2405.13526*, 2024.

810 Alessandro Sperduti and Antonina Starita. Supervised neural networks for the classification of
 811 structures. *IEEE Transactions on Neural Networks*, 8(3), 1997.

812

813 Stevan Stanovic, Benoit Gaüzère, and Luc Brun. Graph neural networks with maximal independent
 814 set-based pooling: Mitigating over-smoothing and over-squashing. *Pattern Recognition Letters*,
 815 187, 2025.

816

817 Qingyun Sun, Jianxin Li, Haonan Yuan, Xingcheng Fu, Hao Peng, Cheng Ji, Qian Li, and Philip S
 818 Yu. Position-aware structure learning for graph topology-imbalance by relieving under-reaching
 819 and over-squashing. In *Proceedings of the 31st ACM International Conference on Information &*
820 Knowledge Management (ICKM), pp. 1848–1857, 2022.

821

822 Jake Topping, Francesco Di Giovanni, Benjamin Paul Chamberlain, Xiaowen Dong, and Michael M.
 823 Bronstein. Understanding over-squashing and bottlenecks on graphs via curvature. In *Proceedings*
824 of the 10th International Conference on Learning Representations (ICLR), 2022.

825

826 Floriano Tori, Vincent Holst, and Vincent Ginis. The effectiveness of curvature-based rewiring
 827 and the role of hyperparameters in GNNs revisited. In *Proceedings of the 13th International*
828 Conference on Learning Representations (ICLR), 2025.

829

830 Domenico Tortorella and Alessio Micheli. Leave graphs alone: Addressing over-squashing without
 831 rewiring. In *The 1st Learning on Graphs Conference (LoG)*, 2022.

832

833 Aafaq Mohi ud din and Shaima Qureshi. Limits of depth: Over-smoothing and over-squashing in
 834 gnns. *Big Data Mining and Analytics*, 7, 2024.

835

836 Hongwei Wang and Jure Leskovec. Combining graph convolutional neural networks and label
 837 propagation. *ACM Transactions on Information Systems*, 40(4), 2021.

838

839 Junfu Wang, Yuanfang Guo, Liang Yang, and Yunhong Wang. Understanding heterophily for graph
 840 neural networks. In *Proceedings of the 41st International Conference on Machine Learning (ICML)*, 2024.

841

842 Keqin Wang, Yulong Yang, Ishan Saha, and Christine Allen-Blanchette. Understanding oversmooth-
 843 ing in gnns as consensus in opinion dynamics. *arXiv preprint arXiv:2501.19089*, 2025.

844

845 Felix Wu, Amauri Souza, Tianyi Zhang, Christopher Fifty, Tao Yu, and Kilian Weinberger. Sim-
 846 plifying graph convolutional networks. In *Proceedings of the 36th International Conference on*
847 Machine Learning (ICML), 2019.

848

849 Xinyi Wu, Amir Ajourlou, Zihui Wu, and Ali Jadbabaie. Demystifying oversmoothing in attention-
 850 based graph neural networks. In *Proceedings of the 37th Conference on Advances in Neural*
851 Information Processing Systems (NeurIPS), 2023a.

852

853 Xinyi Wu, Zhengdao Chen, William Wei Wang, and Ali Jadbabaie. A non-asymptotic analysis of
 854 oversmoothing in graph neural networks. In *Proceedings of the 11th International Conference on*
855 Learning Representations (ICLR), 2023b.

856

857 Keyulu Xu, Chengtao Li, Yonglong Tian, Tomohiro Sonobe, Ken-ichi Kawarabayashi, and Stefanie
 858 Jegelka. Representation learning on graphs with jumping knowledge networks. In *Proceedings of*
859 the 35th International Conference on Machine Learning (ICML), 2018.

860

861 Keyulu Xu, Weihua Hu, Jure Leskovec, and Stefanie Jegelka. How powerful are graph neural
 862 networks? In *Proceedings of the 7th International Conference on Learning Representations*
863 (ICLR), 2019.

864

865 Chaoqi Yang, Ruijie Wang, Shuochao Yao, Shengzhong Liu, and Tarek Abdelzaher. Revisiting
 866 over-smoothing in deep gcns. *arXiv preprint arXiv:2003.13663*, 2020.

867

868 Wenhang Yu, Xueqi Ma, James Bailey, Yibing Zhan, Jia Wu, Bo Du, and Wenbin Hu. Graph
 869 structure reforming framework enhanced by commute time distance for graph classification.
870 Neural Networks, 168, 2023.

864 Kaicheng Zhang, Piero Deidda, Desmond Higham, and Francesco Tudisco. Rethinking oversmoothing
 865 in graph neural networks: A rank-based perspective. *arXiv preprint arXiv:2502.04591*, 2025.
 866

867 Wentao Zhang, Zeang Sheng, Ziqi Yin, Yuezihan Jiang, Yikuan Xia, Jun Gao, Zhi Yang, and Bin Cui.
 868 Model degradation hinders deep graph neural networks. In *Proceedings of the 28th ACM SIGKDD
 869 Conference on Knowledge Discovery and Data Mining (KDD)*, 2022.

870 Xuan Zhang, Limei Wang, Jacob Helwig, Youzhi Luo, Cong Fu, Yaochen Xie, Meng Liu, Yuchao
 871 Lin, Zhao Xu, Keqiang Yan, et al. Artificial intelligence for science in quantum, atomistic, and
 872 continuum systems. *arXiv preprint arXiv:2307.08423*, 2023.
 873

874 Lingxiao Zhao and Leman Akoglu. Pairnorm: Tackling oversmoothing in gnns. In *Proceedings of
 875 the 8th International Conference on Learning Representations (ICLR)*, 2020.

876 Yilun Zheng, Sitao Luan, and Lihui Chen. What is missing in homophily? disentangling graph
 877 homophily for graph neural networks. *arXiv preprint arXiv:2406.18854*, 2024.
 878

879 Kaixiong Zhou, Xiao Huang, Yuening Li, Daochen Zha, Rui Chen, and Xia Hu. Towards deeper graph
 880 neural networks with differentiable group normalization. In *Proceedings of the 34th Conference
 881 on Advances in Neural Information Processing Systems (NeurIPS)*, 2020.

882 Kaixiong Zhou, Xiao Huang, Daochen Zha, Rui Chen, Li Li, Soo-Hyun Choi, and Xia Hu. Dirichlet
 883 energy constrained learning for deep graph neural networks. In *Proceedings of the 35th Conference
 884 on Advances in Neural Information Processing Systems (NeurIPS)*, 2021.
 885

886 Jiong Zhu, Yujun Yan, Lingxiao Zhao, Mark Heimann, Leman Akoglu, and Danai Koutra. Beyond
 887 homophily in graph neural networks: Current limitations and effective designs. In *Proceedings of
 888 the 34th Conference on Neural Information Processing Systems (NeurIPS)*, 2020.
 889

890

891

892

893

894

895

896

897

898

899

900

901

902

903

904

905

906

907

908

909

910

911

912

913

914

915

916

917

918 A TABLE OF COMMON BELIEFS WITH REFERENCES
919920 Table 2: List of common beliefs together with a non-exhaustive list of papers that make those claims.
921

Common Belief and references	
1. OSM is the cause of performance degradation.	
925 926 927 928 929 930 931 932 933 934 935 936 937 938 939 940 941 942 943 944 945 946 947 948 949 950 951 952 953 954 955 956 957 958 959 960 961 962 963 964 965 966 967 968 969 970 971	<p>(Li et al., 2018; Hamilton, 2020; Cai & Wang, 2020; Chen et al., 2020b;a; Hasanzadeh et al., 2020; Huang et al., 2020; Liu et al., 2020; Rong et al., 2020; Zhao & Akoglu, 2020; Zhou et al., 2020; Wang & Leskovec, 2021; Zhou et al., 2021; Bodnar et al., 2022; Chen et al., 2022; Hwang et al., 2022; Rusch et al., 2022; Tortorella & Micheli, 2022; Cai et al., 2023; Maskey et al., 2023; Nguyen et al., 2023; Karhadkar et al., 2023; Rusch et al., 2023; ud din & Qureshi, 2024; Wu et al., 2023a; Epping et al., 2024; Jamadandi et al., 2024; Roth & Liebig, 2024; Stanovic et al., 2025; Wang et al., 2025)</p>
2. OSM is a property of all DGNs.	
925 926 927 928 929 930 931 932 933 934 935 936 937 938 939 940 941 942 943 944 945 946 947 948 949 950 951 952 953 954 955 956 957 958 959 960 961 962 963 964 965 966 967 968 969 970 971	<p>(Xu et al., 2018; Gasteiger et al., 2019; Li et al., 2019; Chen et al., 2020b; Hamilton, 2020; Hasanzadeh et al., 2020; Huang et al., 2020; Zhao & Akoglu, 2020; Zhou et al., 2020; Alon & Yahav, 2021; Zhou et al., 2021; Abboud et al., 2022; Arnaiz-Rodriguez et al., 2022; Chen et al., 2022; Hwang et al., 2022; Keriven, 2022; Topping et al., 2022; Rusch et al., 2022; Akansha, 2023; Cai et al., 2023; Di Giovanni et al., 2023a; Errica et al., 2025; Giraldo et al., 2023; Nguyen et al., 2023; ud din & Qureshi, 2024; Rusch et al., 2023; Shao et al., 2023; Wu et al., 2023a;b; Attali et al., 2024a;b; Fesser & Weber, 2024; Jamadandi et al., 2024; Roth & Liebig, 2024; Arroyo et al., 2025; Wang et al., 2025)</p>
3. Homophily is good, heterophily is bad.	
925 926 927 928 929 930 931 932 933 934 935 936 937 938 939 940 941 942 943 944 945 946 947 948 949 950 951 952 953 954 955 956 957 958 959 960 961 962 963 964 965 966 967 968 969 970 971	<p>(Pei et al., 2020; Zhou et al., 2020; Zhu et al., 2020; Lim et al., 2021; Luan et al., 2021; Wang & Leskovec, 2021; Arnaiz-Rodriguez et al., 2022; Bodnar et al., 2022; Di Giovanni et al., 2023b; Liu et al., 2023b; Platonov et al., 2023a; Bi et al., 2024; Attali et al., 2024a;b; Gong et al., 2024; Roth & Liebig, 2024; Zheng et al., 2024)</p>
4. Long-range propagation is evaluated on heterophilic graphs.	
925 926 927 928 929 930 931 932 933 934 935 936 937 938 939 940 941 942 943 944 945 946 947 948 949 950 951 952 953 954 955 956 957 958 959 960 961 962 963 964 965 966 967 968 969 970 971	<p>(Arnaiz-Rodriguez et al., 2022; Tortorella & Micheli, 2022; Akansha, 2023; Black et al., 2023; Maskey et al., 2023; Huang et al., 2024; Giraldo et al., 2023; Attali et al., 2024a; Tori et al., 2025)</p>
5. Different classes imply different features.	
925 926 927 928 929 930 931 932 933 934 935 936 937 938 939 940 941 942 943 944 945 946 947 948 949 950 951 952 953 954 955 956 957 958 959 960 961 962 963 964 965 966 967 968 969 970 971	<p>(Abu-El-Haija et al., 2019; Pei et al., 2020; Lim et al., 2021; Luan et al., 2021; Ma et al., 2022; Sun et al., 2022; Luan et al., 2022; Rusch et al., 2023; Attali et al., 2024a;b; Bi et al., 2024; Huang et al., 2024; Wang et al., 2024; Zheng et al., 2024)</p>
6. OSQ synonym of a topological bottleneck.	
925 926 927 928 929 930 931 932 933 934 935 936 937 938 939 940 941 942 943 944 945 946 947 948 949 950 951 952 953 954 955 956 957 958 959 960 961 962 963 964 965 966 967 968 969 970 971	<p>(Xu et al., 2018; Arnaiz-Rodriguez et al., 2022; Banerjee et al., 2022; Chen et al., 2022; Deac et al., 2022; Sun et al., 2022; Topping et al., 2022; Tortorella & Micheli, 2022; Akansha, 2023; Balla, 2023; Black et al., 2023; Di Giovanni et al., 2023a; Errica et al., 2025; Gabrielsson et al., 2023; Giraldo et al., 2023; Karhadkar et al., 2023; Liu et al., 2023a; Nguyen et al., 2023; Shao et al., 2023; Shi et al., 2023; ud din & Qureshi, 2024; Yu et al., 2023; Attali et al., 2024a;b; Barbero et al., 2024; Di Giovanni et al., 2024; Fesser & Weber, 2024; Huang et al., 2024; Jamadandi et al., 2024; Southern et al., 2024; Arroyo et al., 2025; Gravina et al., 2025; Stanovic et al., 2025; Tori et al., 2025)</p>
7. OSQ synonym of computational bottleneck.	
925 926 927 928 929 930 931 932 933 934 935 936 937 938 939 940 941 942 943 944 945 946 947 948 949 950 951 952 953 954 955 956 957 958 959 960 961 962 963 964 965 966 967 968 969 970 971	<p>(Alon & Yahav, 2021; Abboud et al., 2022; Arnaiz-Rodriguez et al., 2022; Banerjee et al., 2022; Chen et al., 2022; Deac et al., 2022; Sun et al., 2022; Topping et al., 2022; Tortorella & Micheli, 2022; Akansha, 2023; Black et al., 2023; Dwivedi et al., 2022; Errica et al., 2025; Giraldo et al., 2023; Gutteridge et al., 2023; Nguyen et al., 2023; Karhadkar et al., 2023; Shao et al., 2023; Shi et al., 2023; ud din & Qureshi, 2024; Attali et al., 2024a;b; Barbero et al., 2024; Di Giovanni et al., 2024; Fesser & Weber, 2024; Huang et al., 2024; Jamadandi et al., 2024; Southern et al., 2024; Attali et al., 2024b; Arroyo et al., 2025; Gravina et al., 2025; Stanovic et al., 2025)</p>
8. OSQ problematic for long-range tasks.	
925 926 927 928 929 930 931 932 933 934 935 936 937 938 939 940 941 942 943 944 945 946 947 948 949 950 951 952 953 954 955 956 957 958 959 960 961 962 963 964 965 966 967 968 969 970 971	<p>(Alon & Yahav, 2021; Abboud et al., 2022; Banerjee et al., 2022; Chen et al., 2022; Deac et al., 2022; Topping et al., 2022; Tortorella & Micheli, 2022; Akansha, 2023; Black et al., 2023; Cai et al., 2023; Di Giovanni et al., 2023a; Errica et al., 2025; Gabrielsson et al., 2023; Karhadkar et al., 2023; Nguyen et al., 2023; Liu et al., 2023a; Shi et al., 2023; Yu et al., 2023; Barbero et al., 2024; Di Giovanni et al., 2024; Fesser & Weber, 2024; Huang et al., 2024; Southern et al., 2024; Attali et al., 2024b; Arroyo et al., 2025; Gravina et al., 2025; Stanovic et al., 2025)</p>
9. Topological bottlenecks associated with long-range problems.	
925 926 927 928 929 930 931 932 933 934 935 936 937 938 939 940 941 942 943 944 945 946 947 948 949 950 951 952 953 954 955 956 957 958 959 960 961 962 963 964 965 966 967 968 969 970 971	<p>(Topping et al., 2022; Tortorella & Micheli, 2022; Akansha, 2023; Black et al., 2023; Karhadkar et al., 2023; Liu et al., 2023a; Shi et al., 2023; Fesser & Weber, 2024)</p>

972 **B BACKGROUND**
973974 **B.1 DEEP GRAPH NETWORKS**
975976 We provide a brief excursus into Deep Graph Networks for readers new to the topic.
977978 We can define a graph as a tuple $g = (\mathcal{V}_g, \mathcal{E}_g, \mathcal{X}_g, \mathcal{A}_g)$, with \mathcal{V}_g the set of nodes, \mathcal{E}_g the set of edges
979 (oriented or not oriented) connecting pairs of nodes. \mathcal{E}_g encodes the topological information of the
980 graph and can be represented as an adjacency matrix: a binary square matrix \mathbf{A} where \mathbf{A}_{uv} is 1 if
981 there is an edge between u and v , and it is 0 otherwise. Additional node and edge features belong are
982 represented by $\mathbf{x}_v \in \mathcal{X}_g$ and $\mathbf{a}_{uv} \in \mathcal{A}_g$, respectively. \mathcal{X}_g can be, for instance, \mathbb{R}^d , $d \in \mathbb{N}^+$.
983983 The neighborhood of a node v is the set of nodes that are connected to v by an oriented edge, i.e.,
984 $\mathcal{N}_v = \{u \in \mathcal{V}_g | (u, v) \in \mathcal{E}_g\}$. If the graph is undirected, we convert each non-oriented edge into two
985 oriented but opposite ones.
986986 The main mechanism of DGNs is the repeated aggregation of neighbors' information, which gives
987 rise to the spreading of local information across the graph. The process is simple: i) at iteration ℓ ,
988 each node receives "messages" (usually just node representations) from the neighbors and processes
989 them into a single new message; ii) the message is used to update the representation of that node.
990 Both steps involve learnable functions, so DGNs can learn to capture the relevant correlations in the
991 graph.
992992 Most DGNs implement a synchronous message-passing mechanism, meaning each node always
993 receives information from all neighbors at every iteration step. This local and iterative processing
994 is at the core of DGNs' efficiency since computation can be easily parallelized across nodes. In
995 addition, being local means being independent of the graph's size. When one learns the same function
996 for all message passing iterations, we talk about *recurrent* architectures, as the GNN of Gori et al.
997 (2005); Scarselli et al. (2009); on the contrary, when one learns a separate parametrization for a finite
998 number of iterations (also known as layers), we talk about *convolutional* architectures as the NN4G
999 of Micheli & Sestito (2005); Micheli (2009).
10001000 The neighborhood aggregation is usually implemented using permutation-invariant functions, which
1001 make learning possible on cyclic graphs that have no consistent topological ordering of their nodes.
1002 A rather general and classical neighborhood aggregation mechanism for node v at layer/step $\ell + 1$ is
1003 the following:
1004

1005
$$\mathbf{h}_v^{\ell+1} = \phi^{\ell+1} \left(\mathbf{h}_v^\ell, \Psi(\{\psi^{\ell+1}(\mathbf{h}_u^\ell) \mid u \in \mathcal{N}_v\}) \right) \quad (3)$$

1006

1007 where \mathbf{h}_u^ℓ is the node embedding of u at layer/step ℓ , ϕ and ψ implement learnable functions, and
1008 Ψ is a permutation invariant aggregation function. Note that $\mathbf{h}_v^0 = \mathbf{x}_v$. For instance, the Graph
1009 Convolutional Network of Kipf & Welling (2017) implements the following aggregation, which is a
1010 special case of the above equation:
1011

1012
$$\mathbf{h}_v^{\ell+1} = \sigma(\mathbf{W}^{\ell+1} \sum_{u \in \mathcal{N}(v)} \hat{\mathbf{L}}_{uv} \mathbf{h}_u^\ell), \quad (4)$$

1013

1014 with $\hat{\mathbf{L}}$ being the normalized graph Laplacian, \mathbf{W} is a learnable weight matrix and σ is a non-linear
1015 activation function.
10161017 **B.2 SOME OSM DEFINITIONS**
10181019 In order to keep the paper self-contained and to illustrate the different ways OSM has been defined,
1020 we briefly review the most common definitions. The following subsection summarizes the most
1021 commonly used OSM metrics. Some of these metrics are used in the main text.
10221023 Let $D = \text{diag}(d_1, \dots, d_n)$ be the degree matrix with $d_u = \sum_v A_{uv}$. The combinatorial graph
1024 Laplacian is defined as $\mathbf{L} = \mathbf{D} - \mathbf{A}$, with eigenvalues $0 = \lambda_1 \leq \lambda_2 \leq \dots \leq \lambda_n$. In addition, the
1025 symmetric normalized Laplacian, defined by $\hat{\mathbf{L}} = \mathbf{I} - \mathbf{D}^{1/2} \mathbf{A} \mathbf{D}^{1/2}$, normalizes each entry to remove
1026 the influence of node degrees and its spectrum lies in $[0, 2]$.
1027

1026 DE Chung (1997) was used to measure OSM in Cai & Wang (2020) is defined as
 1027

$$1028 \hat{DE}(\mathbf{H}^\ell) = \text{Tr}((\mathbf{H}^\ell)^T \hat{\mathbf{L}} \mathbf{H}^\ell) = \frac{1}{2} \sum_{u,v \in \mathcal{E}} \left\| \frac{\mathbf{h}_u}{\sqrt{d_u}} - \frac{\mathbf{h}_v}{\sqrt{d_v}} \right\|_2^2 \quad (5)$$

1031 Note that DE can also be computed using \mathbf{L}
 1032

$$1033 DE(\mathbf{H}^\ell) = \text{Tr}((\mathbf{H}^\ell)^T \mathbf{L} \mathbf{H}^\ell) = \frac{1}{2} \sum_{u,v \in \mathcal{E}} \|\mathbf{h}_u - \mathbf{h}_v\|_2^2 \quad (6)$$

1036 Other OSM metrics include with respect to the norm of node embeddings. For instance, Rayleigh
 1037 Quotient (RQ) Chung (1997), which can be seen as normalized DE, is defined by
 1038

$$1039 RQ = \frac{\text{Tr}((\mathbf{H}^\ell)^T \hat{\mathbf{L}} \mathbf{H}^\ell)}{\|\mathbf{H}^\ell\|_F^2} \quad (7)$$

1042 first proposed for OSM analysis in (Cai & Wang, 2020) and later used by (Yang et al., 2020;
 1043 Di Giovanni et al., 2023b; Roth & Liebig, 2024; Maskey et al., 2023). RQ discerns whether
 1044 embeddings become *relatively* smoother, independent of magnitude.

1045 Mean Absolute Deviation (MAD) (Chen et al., 2020a) averages cosine dissimilarity between a node
 1046 and its neighbors.

$$1047 \text{MAD}_G(\mathbf{H}^\ell) = \frac{1}{n} \sum_{v \in \mathcal{V}} \sum_{u \in \mathcal{N}_v} 1 - \frac{\mathbf{h}_v^\ell \mathbf{h}_u^\ell}{\|\mathbf{h}_v^\ell\| \|\mathbf{h}_u^\ell\|} \quad (8)$$

1050 The smoothness metric SMV Liu et al. (2020) captures a global node-distance average over all node
 1051 pairs:
 1052

$$1053 \text{SMV} = \frac{1}{n} \sum_{u \in \mathcal{V}} \frac{1}{n-1} \sum_{v \neq u \in \mathcal{V}} \frac{1}{2} \left\| \frac{\mathbf{h}_u}{\|\mathbf{h}_u\|} - \frac{\mathbf{h}_v}{\|\mathbf{h}_v\|} \right\| \quad (9)$$

1055 In the main text, we primarily consider DE and RQ. However, all notions convey the same intuition,
 1056 loss of discriminative variation, yet, as we show, can disagree in practice.
 1057

1058 **Convergence-rate results.** Known theoretical bounds show $DE(H^k)$ decays exponentially with
 1059 depth k (e.g., the rate depends on weight spectra and graph eigenvalues) (Oono & Suzuki, 2020;
 1060 Huang et al., 2020). Such convergence rate results primarily make assumptions on the architecture,
 1061 weight matrix, and activation functions, and may be altered by skip connections, normalization layers,
 1062 or simple rescaling such as $2W$ (Roth & Liebig, 2024).

1064 For instance Cai & Wang (2020) propose a bound on the DE of two consecutive message passing
 1065 layers (similar bounds found in Oono & Suzuki (2020); Zhou et al. (2021))

$$1066 \hat{DE}(\mathbf{H}^\ell) \leq (1 - \lambda_2)^2 s_{\max}^\ell \hat{DE}(\mathbf{H}^{\ell-1})$$

1068 being s_{\max}^ℓ the square of the maximum singular value of W^ℓ , and λ_2 the second smallest eigenvalue
 1069 of the Laplacian, i.e. the spectral gap. The proof holds when $s_{\max}^\ell < 1/(1 - \lambda_2)$.

1070 In addition, Di Giovanni et al. (2023b) further relate Laplacian eigenvalues and weight spectra to
 1071 explain whether RQ converges to 0 (collapse) or to λ_{\max} (no collapse).

1073 B.3 SOME OSQ DEFINITIONS

1075 For completeness, we summarize some of the most commonly used metrics in the OSQ literature
 1076 and their relationships. These quantities mainly measure three different aspects of the graph: (i)
 1077 *sensitivity/Jacobian* measures that capture how information from a distant node u affects a target
 1078 node v after K message-passing layers; (ii) *topological bottleneck* proxies such as Cheeger-type
 1079 cut ratios, graph spectrum or curvature scores; and (iii) *distance-based* quantities such as effective
 resistance that upper-bound information flow.

1080 B.3.1 SENSITIVITY
1081

1082 For a K -layer GNN let $h_u^{(k)}$ denote the embedding of node u at layer k . A first proxy for OSQ is the
1083 *Influence Score* of Xu et al. (2018),

$$1084 \quad 1085 \quad 1086 \quad I(u, v) = \left\| \frac{\partial \mathbf{h}_u^K}{\partial \mathbf{h}_v^0} \right\|. \quad (10)$$

1087 Black et al. (2023) sum these sensitivities over *all* unordered pairs,

$$1088 \quad 1089 \quad 1090 \quad \sum_{u \neq v \in V} \left\| \frac{\partial \mathbf{h}_u^K}{\partial \mathbf{h}_v^0} \right\|, \quad (11)$$

1091 to obtain a graph-level indicator of how much information is lost.

1092 Di Giovanni et al. (2023b) propose a *symmetric Jacobian obstruction* that removes self-influence and
1093 degree bias. They define the Jacobian obstruction of node v with respect to node u at layer m as

$$1094 \quad 1095 \quad 1096 \quad \tilde{\mathbf{J}}_k^{(m)}(v, u) := \left(\frac{1}{d_v} \frac{\partial \mathbf{h}_v^{(m)}}{\partial \mathbf{h}_v^{(k)}} - \frac{1}{\sqrt{d_v d_u}} \frac{\partial \mathbf{h}_v^{(m)}}{\partial \mathbf{h}_u^{(k)}} \right) + \left(\frac{1}{d_u} \frac{\partial \mathbf{h}_u^{(m)}}{\partial \mathbf{h}_u^{(k)}} - \frac{1}{\sqrt{d_v d_u}} \frac{\partial \mathbf{h}_u^{(m)}}{\partial \mathbf{h}_v^{(k)}} \right), \quad (12)$$

1097 being the extension to the Jacobian obstruction of node v with respect to node u after m layers
1098 defined as

$$1099 \quad 1100 \quad 1101 \quad \tilde{\mathbf{O}}^m(u, v) = \sum_{k=0}^m \left\| \tilde{\mathbf{J}}_k^{(m)}(v, u) \right\|. \quad (13)$$

1102 B.3.2 TOPOLOGICAL BOTTLENECKS
1103

1104 Many OSQ papers measure topological (structural) bottlenecks using spectral or curvature quantities.
1105 Note that here we give an intuition based on the spectral metrics Arnaiz-Rodriguez et al. (2022);
1106 Karhadkar et al. (2023); Banerjee et al. (2022), but a significant part of the literature uses metrics
1107 based on curvature Topping et al. (2022); Liu et al. (2023a); Giraldo et al. (2023); Nguyen et al.
1108 (2023).

1109 First, the topological bottleneck can be measured by Cheeger Constant Chung (1997), which is the
1110 size of the min-cut of the graph.

$$1111 \quad 1112 \quad 1113 \quad h_G = \min_{S \subset V} \frac{|\{e = (u, v) : u \in S, v \in \bar{S}\}|}{\min\{\text{vol}(S), \text{vol}(\bar{S})\}}$$

1114 A small h_G means one can separate G into two large-volume parts by removing only a few edges, i.e.
1115 a severe *topological bottleneck*. Cheeger's inequality links h_G to the spectrum of G :

$$1116 \quad 1117 \quad \frac{h_G^2}{2} \leq \lambda_2 \leq 2h_G,$$

1118 where λ_2 is the second eigenvalue of the normalized Laplacian.

1119 B.3.3 PAIRWISE DISTANCES
1120

1121 The commute time between two nodes Lovász (1993) is defined as the expected number of steps that
1122 a random walker needs to go from node u to v and come back. The Effective Resistance between two
1123 nodes Chandra et al. (1989), R_{uv} , is the commute time divided by the volume of the graph Klein &
1124 Randić (1993), which is the sum of the degrees of all nodes in the graph. The effective resistance
1125 between two nodes is computed as

$$1126 \quad 1127 \quad R_{u,v} = L_{ii}^+ + L_{jj}^+ - 2L_{ij}^+$$

1128 being $\mathbf{L}^+ = \sum_{i>0} \frac{1}{\lambda_i} \phi_i \phi_i^T$ the pseudoinverse of \mathbf{L}

1129 Then, some measures derived from this metric can be connected with the topological bottleneck Chung
1130 (1997); Chandra et al. (1989); Qiu & Hancock (2007). For instance, the maximum effective resistance
1131 of a graph is connected with the Cheeger constant as per $R_{\max} = \max_{u,v \in V} R_{uv}$

$$1132 \quad 1133 \quad R_{\max} \leq \frac{1}{h_G^2}$$

1134 and thus also bounded by the spectral gap as
 1135

$$\frac{1}{n\lambda_2} \leq R_{\max} \leq \frac{2}{\lambda_2}.$$

1138 In addition, the total effective resistance $R_{\text{tot}} = 1/2 \sum_{u,v \in \mathcal{V}} R_{uv}$ is bounded to the spectral gap Ellens
 1139 et al. (2011):
 1140

$$\frac{n}{\lambda_2} \leq R_{\text{tot}} \leq \frac{n(n-1)}{\lambda_2}$$

1141 Note that the total effective resistance also equals the sum of the spectrum of \mathbf{L}^+ $R_{\text{tot}} = n \sum_2^n 1/\lambda_n$.
 1142

1144 B.3.4 CONNECTING SENSITIVITY AND TOPOLOGICAL DISTANCES

1146 The larger Total Effective Resistance ($R_{\text{tot}} = \sum_{(u,v) \in V} R_{uv}$) is, the lower the sum of pairwise
 1147 sensitivities Black et al. (2023):
 1148

$$\sum_{u,v \in V \times V} \left\| \frac{\partial h_v^{(r)}}{\partial h_u^{(0)}} \right\| \leq c(b - R_{\text{tot}}) \quad (14)$$

1152 The larger the Effective Resistance is, the higher the Symmetric Jacobian Obstruction Di Giovanni
 1153 et al. (2023b):
 1154

$$\tilde{\mathbf{O}}^m(u, v) = \sum_{k=0}^m \left\| \tilde{\mathbf{J}}_k^{(m)}(v, u) \right\| \leq c R_{u,v} \quad (15)$$

1157 B.4 COMPUTATIONAL BOTTLENECK

1159 Oversquashing can also be seen through the perspective of the message-passing computational graph:
 1160 each message-passing layer expands the set of nodes whose features can influence a target node. If
 1161 this *receptive field* grows fast, any fixed-width DGN “squash” many signals into a single vector.
 1162

1163 **Receptive Field** Following Chen et al. (2018); Alon & Yahav (2021) the receptive field was defined
 1164 recursively as:
 1165

$$\mathcal{N}_v^K := \mathcal{N}_v^{K-1} \cup \{w \mid w \in \mathcal{N}_u \wedge u \in \mathcal{N}_v^{K-1}\} \quad \text{and} \quad \mathcal{N}_v^1 = \mathcal{N}_v \quad (16)$$

1166 which can be also seen as the set of K -hop neighbors neighbors, i.e. nodes that are reachable from v
 1167 within K hops. The number of nodes in each node’s receptive field can grow exponentially with the
 1168 number of layers $|\mathcal{N}_v^K| = \mathcal{O}(\exp(K))$ Chen et al. (2018). For instance, in a rooted binary tree each
 1169 layer has exactly b^{K-1} new neighbors, so $|\mathcal{N}_v^K| = 1 + b + b^2 + \dots + b^{K-1} = \Theta(b^K)$.
 1170

1171
 1172 When evaluating the actual *computational* graph resulting from message-passing, duplicates matter:
 1173 a node that appears in several branches of the computation tree contributes multiple times, since each
 1174 distinct walk contributes a separate message. We therefore use the multiset notation to define the
 1175 *computational tree* for a node v in Eq. 2, [reproduced here for convenience](#):
 1176

$$\mathcal{M}_v^1 := \mathcal{N}_v, \quad \mathcal{M}_v^K := \mathcal{M}_v^{K-1} \uplus \left\{ \biguplus_{u \in \mathcal{M}_v^{K-1}} \mathcal{N}_u \right\}. \quad (17)$$

1182 Therefore, we defined in Def. 4.1 the *computational bottleneck* of node v as the size of the *computational tree*, $|\mathcal{M}_v^K|$, for a given node v and number of message passing layers K .
 1183

1184 The size of the computational bottleneck (multiset receptive field) at node v , can be computed as:
 1185

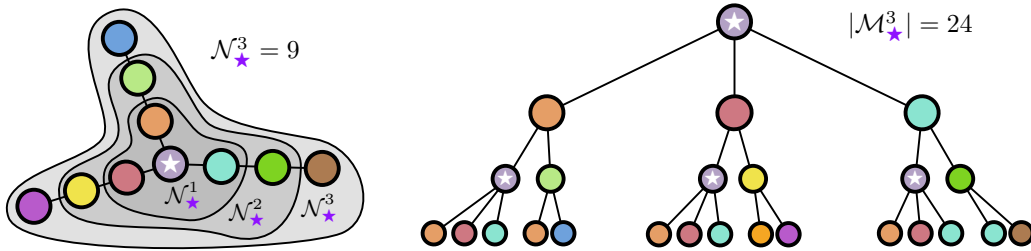
$$|\mathcal{M}_v^K| := \sum_{\ell=1}^K \|A^\ell[v, :] \|_1 = \sum_{\ell=1}^K \sum_{u \in \mathcal{V}} (A^\ell)_{u,v} \quad (18)$$

1188 This definition counts every distinct length- ℓ walk from v to any node u . Equation 18 is
 1189 exactly the row-sum of the powers of the adjacency matrix; it therefore matches the size of the
 1190 *computational tree*.

1191 Note that the size of the set-based receptive field corresponds to the support of the multiset \mathcal{M}_v^K ,
 1192 denoted $\mathcal{N}_v^K := \text{supp}(\mathcal{M}_v^K)$. Therefore, the multiset size $|\mathcal{M}_v^K|$ is always greater than or equal to
 1193 the size of the support, $|\mathcal{N}_v^K| \geq |\mathcal{M}_v^K|$, since it accounts for path multiplicity.

1194 In early deep-graph networks literature, Micheli (2009) introduced the idea by using the term
 1195 “contextual window”: deeper layers aggregate exponentially many paths unless skip connections or
 1196 global pooling curb the growth. The multiset perspective in Eq. 18 makes this explosion
 1197 explicit and the matrix computation directly links to matrix-power interpretations of message passing.

1198 Figure 6 visualises the difference between the set size $|\mathcal{N}_v^K|$ and the multiset size $|\mathcal{M}_v^K|$ on a toy
 1199 graph and on a stochastic block model (SBM).



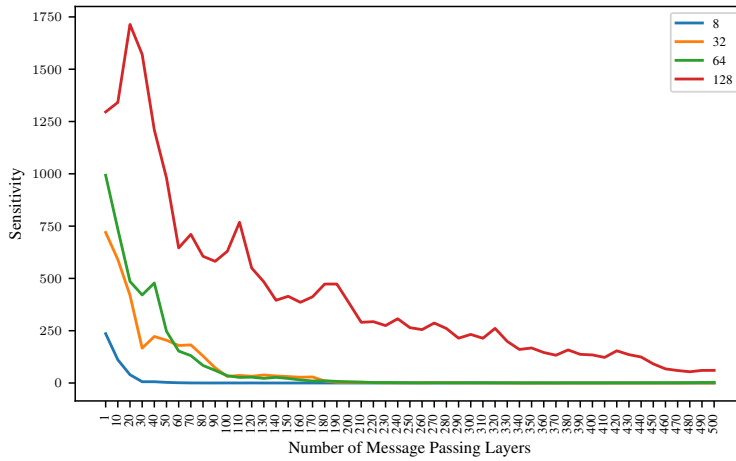
1200
 1201
 1202
 1203
 1204
 1205
 1206
 1207
 1208
 1209
 1210
 1211 **Figure 6: Computational Bottleneck.** Illustration of a receptive field – defined with sets (K -
 1212 hop neighborhood) – and the definition of computational bottleneck measured as the size of the
 1213 computational graph – defined with multisets.

1214 In conclusion, we note that in message-passing, the computational bottleneck is driven not by how
 1215 many distinct vertices are in the K -hop neighborhood, but by the size of the computational graph.

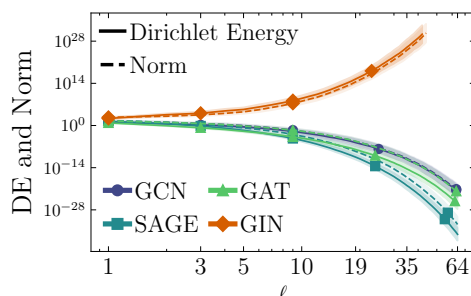
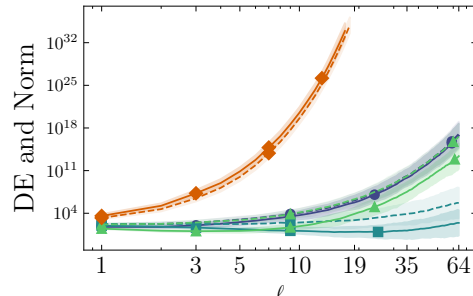
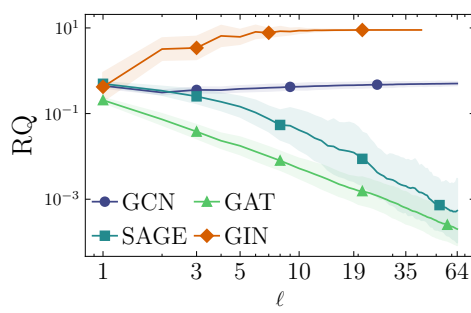
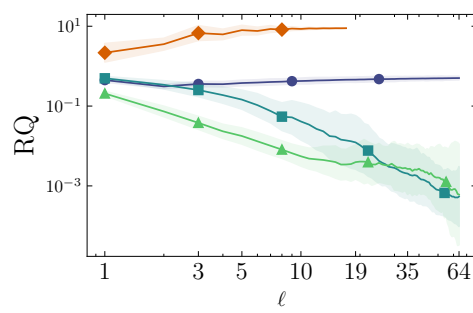
1216
 1217
 1218
 1219
 1220
 1221
 1222
 1223
 1224
 1225
 1226
 1227
 1228
 1229
 1230
 1231
 1232
 1233
 1234
 1235
 1236
 1237
 1238
 1239
 1240
 1241

1242
 1243 **C SENSITIVITY DECREASES ON A GRID GRAPH WITHOUT TOPOLOGICAL**
 1244 **BOTTLENECKS**

1245 To show that low sensitivity does not necessarily imply a topological bottleneck, Figure 7 analyzes
 1246 sensitivity's decreasing trend when the number of message passing layers L increases on the grid
 1247 graph of Figure 4 of size 10×10 . Increasing the size of the embedding space postpones the collapse
 1248 of the sensibility.



1265 Figure 7: We plot the sensitivity of the grid graph of Figure 4 for the Graph Convolutional Network
 1266 Kipf & Welling (2017) model for different node embedding sizes.

1296 D OVERSMOOTHING DOES NOT ALWAYS HAPPEN
12971298 For enhanced clarity and to allow for a more detailed examination of the OSM behavior discussed in
1299 Section 2, a larger version of Figure 1 is provided in Figure 8.
13001311 (a) W : DE and Norm
13121311 (b) $2W$: DE and Norm
13121313 (c) W : RQ
13141313 (d) $2W$: RQ
13141325 Figure 8: **Larger version of Figure 1.** (a-b): We depict the evolution, with increasing number of
1326 layers, of the $DE = \text{tr}(X^T \Delta X)$ and the feature norm $\|X\|_F$, using W and $2W$ feature transformations
1327 for different architectures. (c-d): Evolution of the $RQ = \text{tr}(X^T \Delta X) / \|X\|$ for W and $2W$ as
1328 before. Experiments run on the Cora dataset for 50 random seeds.
1329
1330
1331
1332
1333
1334
1335
1336
1337
1338
1339
1340
1341
1342
1343
1344
1345
1346
1347
1348
1349